Amazonian Moisture Recycling Revisited Using WRF with Water Vapor Tracers

F. Dominguez[1], J. Eiras-Barca[1,2,3], Z. Yang[4], D. Bock[5], R. Nieto[2], and L. Gimeno[2]

[1]Department of Atmospheric Sciences, University of Illinois at Urbana-Champaign. Urbana, IL 61801.
[2]Environmental Physics Laboratory (EPhysLab), CIM-UVIGO, Universidade de Vigo, Ourense, Spain.
[3]Defense University Center at the Spanish Naval Academy, Marín, Spain.
[4]Pacific Northwest National Laboratory, Richland, Washington.
[5]National Center for Supercomputing Applications, University of Illinois at Urbana-Champaign, Urbana, IL,.

Key Points:

- 30% of Amazonian precipitation comes from local evapotranspiration. Local moisture is more efficiently rained out than remote moisture.
- Recycled precipitation shows a strong annual and semi-annual signal, associated with the passage of the Inter-Tropical Convergence Zone.
- A diurnal cycle cycle of Amazonian water vapor reflects the variability of evapotranspiration, recycled precipitation and vapor flux.

Corresponding author: F. Dominguez, `francina@illinois.edu`

Abstract

Previous studies have estimated that 25% to 35% of Amazonian precipitation comes from evapotranspiration (ET) within the basin. However, due to simplifying assumptions of traditional models, these studies primarily focus on large spatial and temporal scales. In this work we use the Weather Research and Forecast (WRF) regional climate model with the added capability of water vapor tracers to track the moisture from Amazonian ET at the native WRF resolution. The tracers reveal that the well-mixed assumption of simpler models does not hold, as local ET is more efficiently rained out of the atmospheric column than remote sources of moisture, particularly in the eastern part of the basin. Recycled precipitation shows a strong annual and semi-annual signal, associated with the passage of the Inter-Tropical Convergence Zone. The tracers also reveal a strong diurnal cycle of Amazonian water vapor related to the diurnal cycle of ET, convective precipitation and advected moisture. ET increases from early morning into the afternoon, some of this moisture is rained out through convective storms in the early evening, while later in the night strong winds associated with the South American Low Level Jet advect moisture downwind. Visualizing the Amazonian water vapor highlights its diurnal beating pattern and suggests that the Amazon has "younger" water than other regions in the globe, with very efficient recycling of local moisture.

Plain Language Summary

Evaporation from soil and transpiration from plants within the Amazon contribute to approximately one third of the precipitation that falls within the basin in a process known as "precipitation recycling". This estimate represents an average over the basin and over many years. In this work we use numerical water tracers within an atmospheric model to quantify precipitation recycling at higher spatial and temporal resolution than previous studies. The tracers allow us to follow the water from the time it evaporates from the land until it falls as precipitation. Our work reveals cycles in water vapor and precipitation of Amazonian origin that had not been previously studied. In particular, the daily timescale shows how evaporation and transpiration increase from early morning into the afternoon and contribute to the accumulation of Amazonian water vapor in the atmosphere. Some of this moisture is rained out in the early evening in convective storms, while later in the night strong winds transport moisture away from the basin. Visualizing the Amazonian water vapor highlights its diurnal beating pattern.

1 Introduction

Early evidence of the importance Amazonian evapotranspiration (ET) for local precipitation came from observational analysis of oxygen-18 (δ^{18}O) in precipitation, which was found to have an inland gradient of δ^{18}O much smaller than in other regions of the world (Salati et al., 1979). This observational result suggested that a significant part of the rainfall came from re-evaporated water, otherwise known as recycled precipitation. Subsequent analyses based on bulk numerical models estimated precipitation recycling (or the percent of precipitation that comes from local ET) ranging from 25%-40% (Brubaker et al., 1993; Eltahir & Bras, 1994; Burde, 2006). There is a strong gradient in recycled precipitation, increasing from east to southwest as the dominant flow enters from the Atlantic Ocean, traverses the basin and encounters the Andes mountains (Eltahir & Bras, 1994; Burde, 2006). It is important to keep in mind that these early bulk models assume that the atmospheric column is well mixed. In other words, they assume that, at the time scales of the model, turbulence effectively mixes the atmosphere so the proportion of precipitation from advected and recycled origin is the same as the proportion found in water vapor. However, early work of Lettau et al. (1979) argued that in a system such as the Amazon it is important to account for fast recycling as diurnal convection yields precipitation before all water vapor from the surface has enough time to mix with the ex-

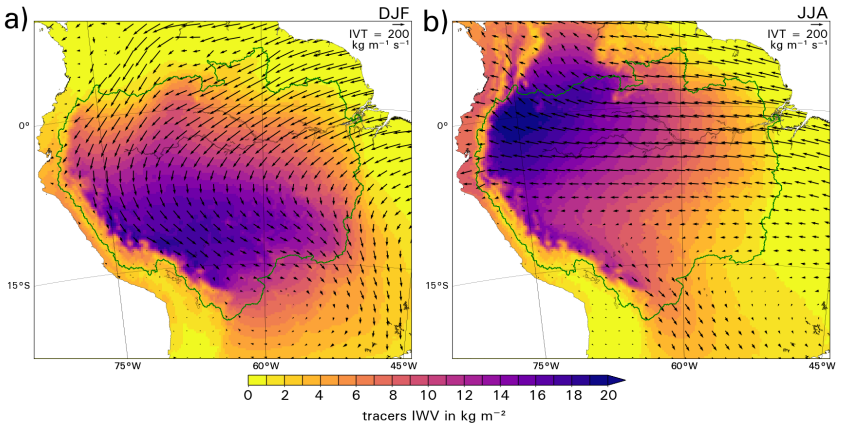

Figure 1. Shading indicates integrated water vapor IWV (kg m^{-2}) of Amazonian origin. Black vectors indicate total integrated vapor transport IVT (kg $m^{-1}s^{-1}$) . Values are average for DJF (a) and JJA (b), for the period 2003-2013.

isting precipitable water in the column. In this sense, moisture from evapotranspiration would be more likely to rain out than advected moisture. When incomplete mixing is taken into account, the bulk model recycling estimates are closer to 45% (Lettau et al., 1979; Burde, 2006). When incorporating incomplete mixing, the spatial distribution of recycling remains similar but the recycling values increase towards the east (Burde, 2006).

Currently, the most physically realistic way to numerically estimate precipitation recycling is using water vapor tracers embedded within atmospheric models, as this method requires the least number of assumptions. Water vapor tracers (WVT) do not make the assumption of a well-mixed atmospheric column used in most bulk models. Embedding tracers within the atmospheric model takes into account the changes in moisture content due to turbulent transport in the planetary boundary layer, cloud microphysics, and convection (Dominguez et al., 2020). Using WVT within a global climate model at a 2° by 2.5° resolution, M. G. Bosilovich and Chern (2006) found a recycling ratio of about 27% in the peak recycling season, a 50% higher value than the estimate using bulk models. This again confirms the idea of "fast recycling" in the Amazon. Interestingly, they found that the inter-annual variability of recycling mostly related to variability in moisture transport, not evapotranspiration. WVT embedded within regional climate models allow us to examine processes at a much higher spatial resolution. Using the WVT embedded within the Weather Research and Forecasting (WRF) model (WRF-WVT), Yang and Dominguez (2019) tracked the water that originated from the Amazon basin to understand how it contributes to precipitation throughout the continent. They found that around 30% of the total precipitation over the Amazon and about 16% of the precipitation in the downwind region of the La Plata River basin originates from Amazonian ET.

All of the work to date has focused on quantifying precipitation recycling over the Amazon at the monthly or longer time scale. However, the dominant processes that affect recycling variability have several characteristic scales of variability. Terrestrial evapotranspiration, which is the source of recycled water vapor, has a strong diurnal cycle. Precipitation in the Amazon is driven by small-scale and organized convection, and also shows a clear diurnal cycle (Tanaka et al., 2014). However, intra-daily time scales of recycled precipitation have not been previously studied in the Amazon because bulk moisture source methods cannot provide information at these time scales due to their under-

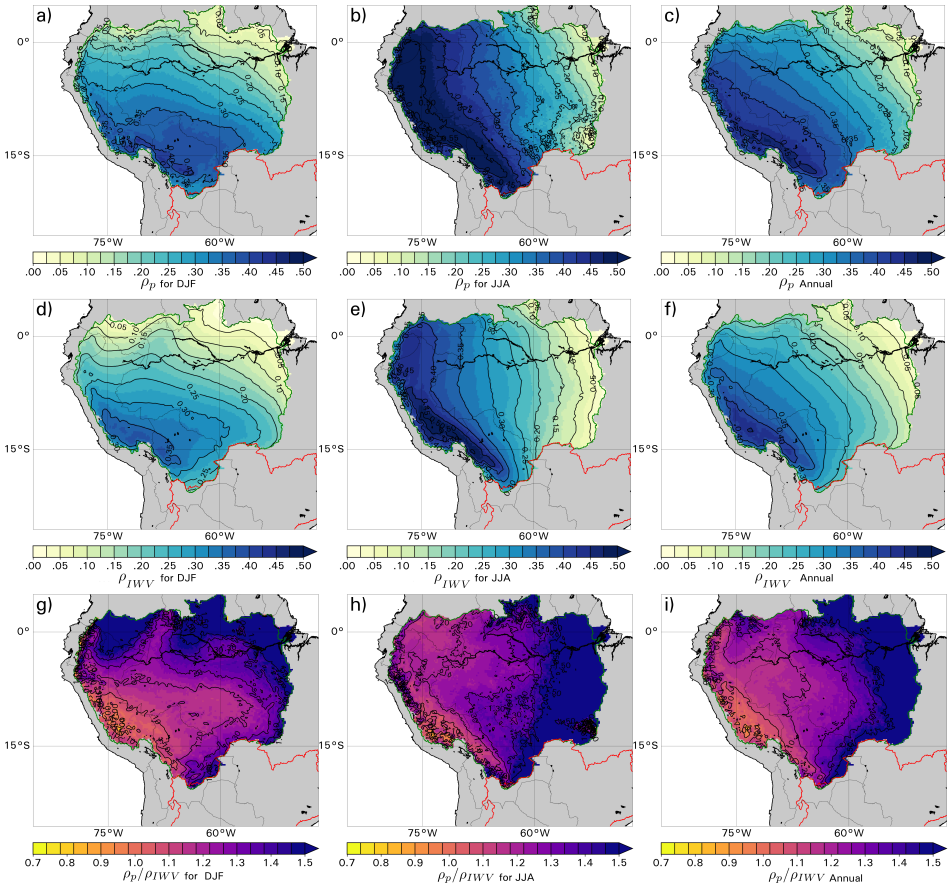

Figure 2. Row 1) Fraction of Amazonian precipitation to total precipitation ($\rho_P = rain_t/rain$) for DJF (a), JJA (b) and Annual means (c). Row 2) Fraction of precipitable water (IWV) of Amazonian origin to total precipitable water ($\rho_{IWV} = IWV_t/IWV$) for DJF (d), JJA (e) and Annual means (f). Row 3) "Precipitation efficiency" (ρ_P/ρ_{IWV}), or row 1 divided by row 2.

lying assumptions. Evidence of the terrestrial signature on the atmosphere at the global scale was highlighted in Tuinenburg and van der Ent (2019) as a daily cycle in the atmospheric residence time of land evaporation which is different from that of water vapor of oceanic sources. A diurnal signature in water vapor would imply much shorter times than the traditional 8-10 day global estimates (van der Ent & Tuinenburg, 2017), or even the recent 4-5 days estimates (Laderach & Sodemann, 2016). WVT-WRF is an ideal tool to study fast turnover processes as it allows us to isolate the terrestrial contributions to atmospheric vapor without having to make assumptions about vertical mixing in the atmosphere. The fact that this is a regional model allows us to delve into the smaller spatial and temporal scales.

In this work we use WRF-WVT to characterize recycling of evapotranspiration over the Amazon. First, results from our analyses are compared to previous work using bulk models. Then, we analyze the characteristic spatial and temporal scales of moisture of Amazonian origin, with particular emphasis on the diurnal timescale.

2 Methods

A 10-year simulation (2003-2013) provided by the mesoscale model WRF (20 km × 20 km) using the entire South American continent as domain of simulation is used here. Water vapor tracers are only available for one set of physics options. As such, the Kain-Fritsch (KF) (Kain & Fritsch, 1990; Kain, 2004) parametrization is used for subgrid-scale convection; the Yonsei University (YSU) (Hong & Pan, 1996) parametrization for turbulent mixing, and the single moment "6-class" (WSM6) (Hong & Lim, 2006) solved the microphysics in phase change and precipitation processes. ERA-Interim (Dee et al., 2011) provides boundary and initial conditions for the simulations.

Two additional tools are used in the WRF simulation to improve the representation of land-atmosphere interactions, as well as provide the ability to track the fate of the Amazonian ET. We used the Noah-Multiparametrization land surface model (Noah-MP LSM) (Niu et al., 2011) with the MMF groundwater scheme developed by Fan et al. (2007) and Miguez-Macho et al. (2007). This scheme is used to take into account the interaction between the shallow aquifers and soil moisture, which affects Amazonian ET, particularly in water limited regions during dry periods (Miguez-Macho & Fan, 2012; Martinez et al., 2016b, 2016a).

We also use the WRF Water Vapor Tracer Tool (WRF-VT) which allows the tracking of the moisture evapotranspired from the Amazon (Dominguez et al., 2016; Eiras-Barca et al., 2017; Insua-Costa & Miguez-Macho, 2018). This moisture can either leave the Amazonian domain or precipitate within the basin (as recycled precipitation). WRF-WVT includes additional output variables related to water vapor and precipitation of tracer origin, as well as other species (see Insua-Costa and Miguez-Macho (2018) for details). In this way, we can calculate the precipitation recycling ratio ($\rho_P = rain_t/rain$) where $rain$ is the total precipitation which includes convective and non-convective processes, while $rain_t$ is the precipitation from Amazonian ET. In a similar way, we can calculate the integrated water vapor (IWV) recycling ratio ($\rho_{IWV} = IWV_t/IWV$). Note that this calculation is done on a cell-by-cell basis. Also note that this method does not require the assumption of a the well-mixed atmosphere in the vertical column that is traditionally used in analytical models such as Brubaker et al. (1993) and Eltahir and Bras (1994). This configuration of WRF was recently used by Eiras-Barca et al. (2020) to an-

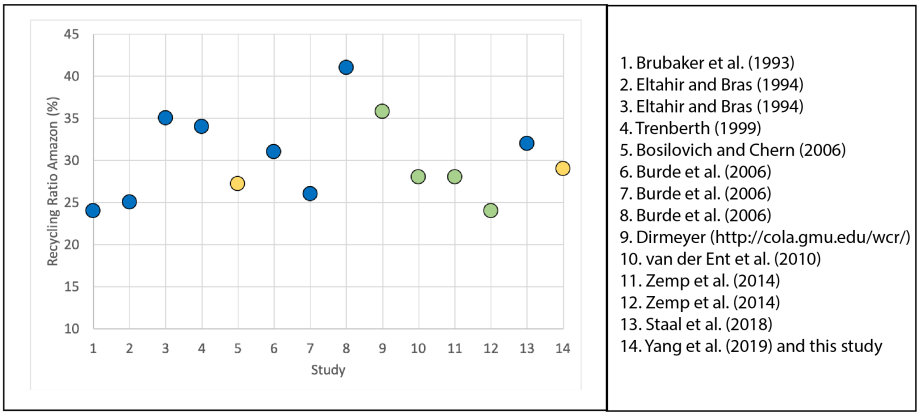

Figure 3. Amazonian climatological recycling ratio as estimated in previous studies which using bulk models (blue), offline models (green) and online models (yellow) to estimate the recycling ratio in the Amazon basin.

alyze the impacts of a realistic future deforestation scenario over the same domain, and a comprehensive validation of these simulations can also be found in Yang and Dominguez (2019). Along with the mean time series obtained with the WRF-VT we also plot the equivalent observations obtained with ERA5 and TRMM (3B42 subset, Huffman et al. (2010)). This helps evaluate WRF's ability to represent the annual and diurnal cycles of the variables of interest.

To extract the dominant signals in the time series of total and tracer ET, precipitation, IWV and IVT we use fast Fourier transform analysis (FFT). Using the 10-year time series, area-averaged over the Amazon basin, the FFT allows us to identify and quantify the strength of the dominant modes with daily to annual periodicity (Wilks, 2011). However, we cannot extract interannual signals with this short timeseries.

3 Results

The moisture transpired by the vegetation and evaporated from the soil of the Amazon basin is carried by the prevalent winds. These winds change dramatically depending on the season. During the Austral summer (DJF), moisture laden winds enter from the tropical North Atlantic Ocean (Drumond et al., 2014), cross the Amazon and travel in a southwesterly direction until they encounter the Andes Mountains and are forced to veer south and east toward southeastern South America (Satyamurty et al., 2013; Segura, 2019). The moisture of Amazonian origin accumulates along the southwest of the Amazon basin (Fig. 1a). During the Austral winter, the trade winds traverse the Amazon in a much more zonal direction, and veer northwest toward Colombia and Venezuela. Moisture of Amazonian origin accumulates along the western and northwestern part of the basin (Fig. 1b). The autumn (March-May, MAM) and spring (September-November, SON) seasons have characteristics that reflect the transition between the Austral winter and summer, these can be found in supplementary material (Fig. S1).

The fraction of precipitation of Amazonian origin to total precipitation (recycling ratio) follows this same spatial pattern, increasing gradually from the Atlantic coast to around 40% in the southwest part of the basin during DJF (Fig. 2a). Interestingly, the recycling ratio is higher during the dry season (JJA) when more than 50% of the precipitation along the eastern Andes is of Amazonian origin (Fig 2b). The corresponding plot for the transitional months (MAM and SON) can be found in Fig. S2. If we analyze recycled to total precipitable water (IWV), the pattern is similar to that of the recycled precipitation, but smaller in magnitude (Fig. 2d-f). This implies that local precipitable water is more efficiently rained out of the atmospheric column than advected moisture. This is likely due to the fact that the moisture for convection is sourced from lower levels, as argued by Lettau et al. (1979). The geographical pattern of efficiency, defined as ρ_P/ρ_{IWV} shows higher efficiencies in the eastern part of the basin, and efficiencies close to one in the west along the Andes. Efficiencies close to one indicate that the atmosphere is well mixed (Eltahir & Bras, 1994). Higher efficiencies in the east indicate that low-level moisture is rained out before it has fully mixed in the atmosphere. In these regions of poor mixing, lower-level humidity experiences an efficient ascent mechanism that leads to precipitation. However, as stated before, the assumption of a well-mixed atmosphere is common among bulk recycling models (Brubaker et al., 1993; Eltahir & Bras, 1994; Dominguez et al., 2006). As seen in Fig. 2 g-i, this assumption is not valid throughout the domain and would result in an under-estimation of recycled precipitation, particularly in the eastern part of the region. However, recycling values in the east are significantly smaller than in the west, so the area-average differences are not as large. We find that area-average annual precipitation recycling is 29%. This compares well with the results from studies using bulk models, offline models and online models (Brubaker et al., 1993; Eltahir & Bras, 1994; Trenberth, 1999; M. Bosilovich & Chern, 2006; Burde, 2006; van der Ent et al., 2010; Zemp et al., 2014; Staal et al., 2018; Yang & Dominguez, 2019) as shown in Figure 3. In all but one study, Amazonian recycling ranges between

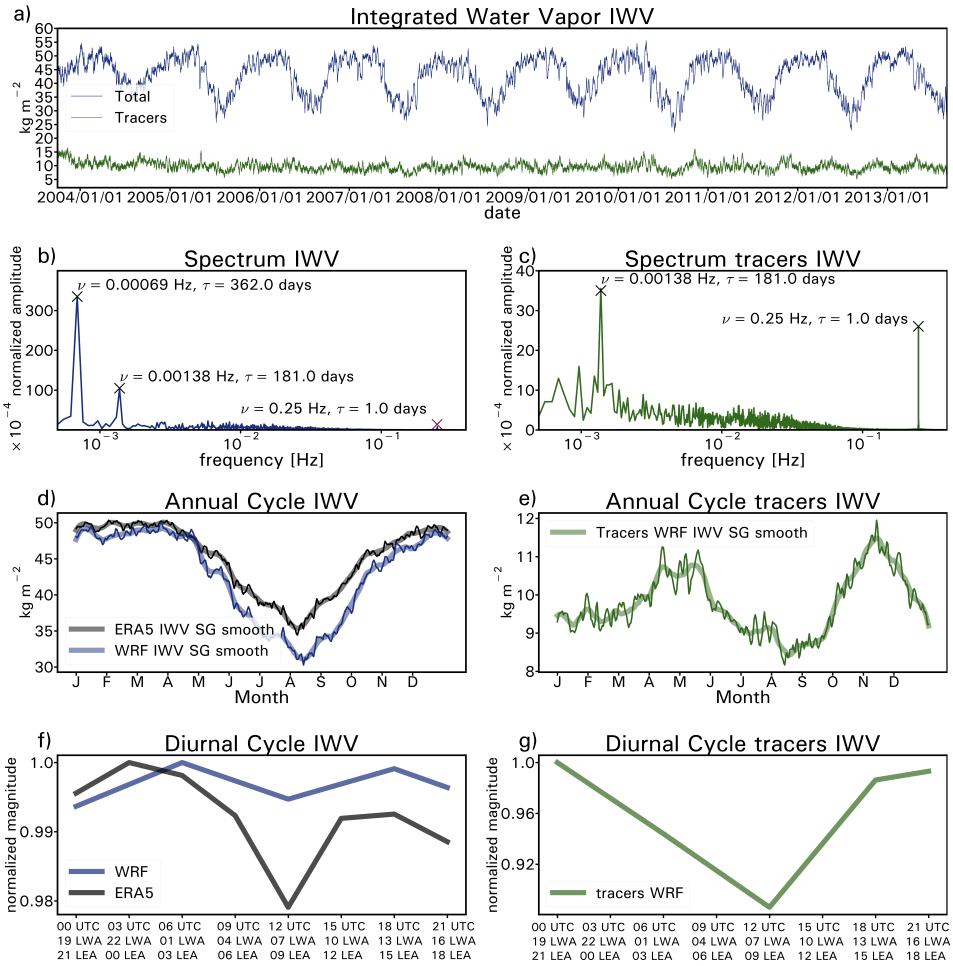

Figure 4. Fast-Fourier transform (FFT) analysis of IWV. a) Raw signals of total IWV (blue) and tracers IWV (green) for a 6h-time step time series 2003-2013. b and c) FFT frequencies spectrum for total IWV (blue) and tracers IWV (green). d) Mean annual cycle for IWV as obtained from the WRF simulations (blue) and ERA5 reanalysis (black). e) Mean annual cycle for tracers IWV as obtained from WRF. f) Mean diurnal cycle for IWV as obtained from the WRF simulations (blue) and ERA5 reanalysis (black). g) Mean diurnal cycle for tracers IWV as obtained from WRF. Note that a Savitzky-Golay (SG) smooth filtered signal is also plotted along with the raw data to ease the visualization when necessary.

25-35%. This result is rather surprising given the large differences in the methods and data sources used. The results also agree with previous analyses in terms of spatial pattern. In particular, those of Eltahir and Bras (1994) using a very simplified two-dimensional model that assumes a well-mixed atmosphere, and atmospheric data at a 2.5° resolution (compared to the three dimensional 20 km resolution of our analyses).

3.1 Temporal Analysis

Using FFT analysis, we find that the characteristic timescale of total IWV has a very clear annual cycle, with a maximum during the Austral summer and a minimum during the winter (blue line Fig. 4a and 4b). The annual signal of WRF is very simi-

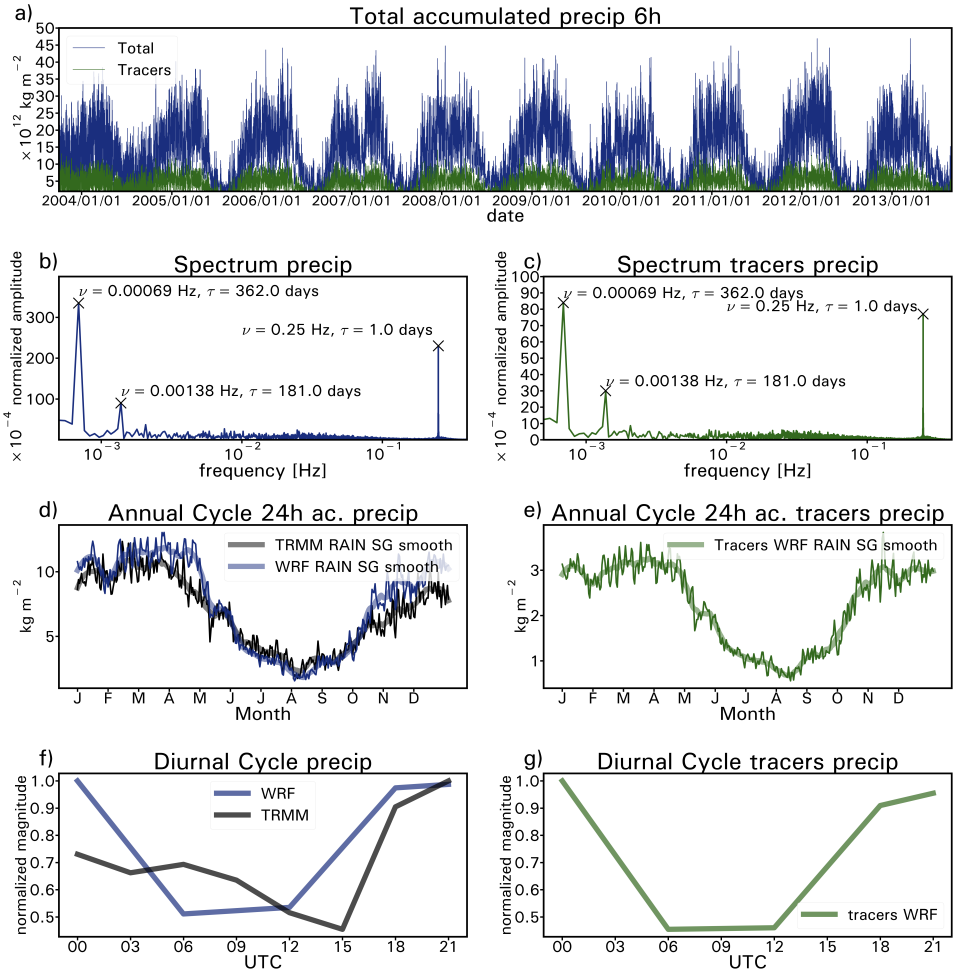

Figure 5. Fast-Fourier transform (FFT) analysis of Precipitation (P) a) Raw signals of total P (blue) and tracers P (green) for a 6h-time step time series 2003-2013. b and c) FFT frequency spectrum for total P (blue) and tracers P (green). d) Mean annual cycle for P as obtained from the WRF simulations (blue) and ERA5 reanalysis (black). e) Mean annual cycle for tracers P as obtained from WRF. f) Mean diurnal cycle for P as obtained from the WRF simulations (blue) and ERA5 reanalysis (black). g) Mean diurnal cycle for tracers P as obtained from WRF.

lar to that of ERA5 (Fig. 4d) . We see another signal with a periodicity of around 6 months (181 days). This signal is due to the migration of the ITCZ, which reaches its southernmost extent in the Austral summer and its northern-most extent during the Boreal summer. The central Amazon basin experiences a peak in IWV as the ITCZ migrates north, and another peak as the ITCZ migrates south. WRF shows a very weak diurnal cycle in total IWV (Fig. 4f), while ERA5 has a slightly stronger diurnal cycle with minimum IWV around 12Z (8am local) and increasing values as the day progresses and a maximum around 3Z (11pm local).

Unlike total IWV, tracer IVW (or water vapor of Amazonian origin) does not show the annual signal, however, it does have the 6-month signal associated to the ITCZ passage (green line in Fig. 4a and c). The six-month signal has a peak from late April to early June, and another peak from October to early December (Fig. 4e). In addition, there is a very clear diurnal signal (Fig. 4c). Figure S3 in the supplementary material

shows the 50th and 80th percentile contours of daily mean tracers IWV corresponding to 00, 06, 12 and 18 UTC. Despite the fact that the static representation provided by the figure does not allow a full appreciation of the diurnal cycle, the position of these percentiles varies significantly throughout the day. The tracer IWV signal generates a pattern that can be clearly seen when visualizing the data as a movie: `https://www.youtube.com/watch?v=sVP9B_85jfw`. We can think of this signal as "the heartbeat of the Amazon". Tracer water vapor is minimum in the early morning and maximum in the late afternoon and evening (Fig. 4g). The physical processes that give rise to characteristic signals in integrated water vapor are due to the sources and sinks of atmospheric moisture: precipitation, evapotranspiration and moisture advection. In the analysis that follows we will focus on each of these sources and sinks.

Total precipitation and recycled precipitation show the same characteristic time scales of variability: annual, 6-month and diurnal (Fig. 5). This implies that the same physical processes that give rise to total precipitation affect recycled precipitation. Total precipitation peaks during the warmer months (Nov-April), with a slight lull in February as the ITCZ is located south and the northern Amazon has a decrease in precipitation (Fig. 5d and Eiras-Barca et al. (2020) Fig. 4). The WRF annual cycle of precipitation coincides with that of TRMM estimates. Tracer precipitation shows a strong annual cycle that was not clear for IVW (compare Figure 5c and 4c). Note that the annual and semi-annual cycle in precipitation has also been detected in the tropical Andes mountains (Segura, 2019), in particular, the authors find a strong semi-annual cycle along the transition zone between the southern and equatorial Andes.

Total precipitation shows a much stronger diurnal cycle than IWV (compare Fig 5b and 4b). The diurnal cycle of precipitation in the Amazon is well known. Hourly station data from the Manaus area shows that precipitation frequency peaks in the afternoon between 14 and 17 local time, and this agrees with remote sensing estimates (Tanaka et al., 2014). It is important to highlight, however, that the diurnal peak depends on the type of precipitation. Late afternoon and early evening peaks are associated with non-mesoscale convective system (MCS) precipitation, while MCS precipitation tends to peak in the early morning (Wu & Lee, 2019). When looking at the overall convective precipitation in the Amazon, regardless of type, we see a peak in the late afternoon and evening, as shown in the TRMM estimates (5f). Precipitation derived from TRMM shows a strong peak between 18-21Z (14-17 local). WRF total and tracer precipitation shows a similar afternoon peak, but sustains the precipitation until around 0z (8pm) which is not seen in the remote sensing estimates.

IVT combines the effect of winds and water vapor (Fig. 6). We see that total IVT is dominated by the annual cycle, as warm season IVT is larger than during the cooler months. This coincides with previous results of Satyamurty et al. (2013) who found that moisture convergence in the basin accounts for most of the rainy season precipitation. High IVT also coincides with the intensification of the South American low-level jet (SALLJ), which transports moisture from the tropics into higher latitudes (Salio et al., 2002; Arraut et al., 2012). Interestingly total IVT shows a stronger diurnal cycle than IWV (Compare Figs 6b and 4b). This highlights the strong diurnal cycle of winds, and its effect on IVT variability. The diurnal cycle of IVT is also closely related to the diurnal cycle of the SALLJ, as has been shown in observations (Vera et al., 2006). Tracer IVT is noisier, with several peaks in addition to the diurnal peak (Fig. 6c). Interestingly, tracer IVT shows intensification during the summer and winter months, indicating that despite lower tracer IWV in the winter, the winds play an important role in moisture transport (Fig. 6d). The diurnal cycle shows weaker IVT between 18Z and 0Z (14-20 local time) as boundary layer turbulence weakens horizontal winds. Higher IVT during the night and early morning would correspond to a stable boundary layer and higher wind speed. Tracer IVT also shows a similar diurnal cycle.

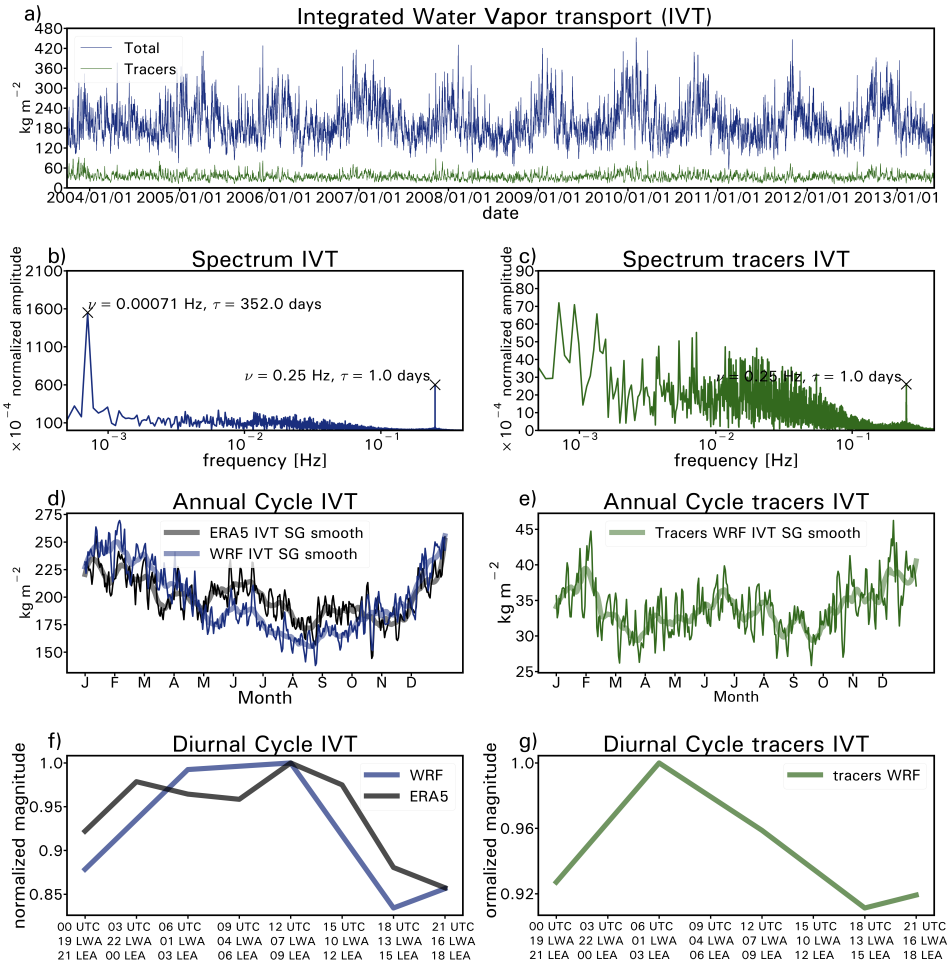

Figure 6. Fast-Fourier transform (FFT) analysis of IVT a) Raw signals of total IVT (blue) and tracers IVT (green) for a 6h-time step time series 2003-2013. b and c) FFT frequencies spectrum for total IVT (blue) and tracers IVT (green). d) Mean annual cycle for IVT as obtained from the WRF simulations (blue) and ERA5 reanalysis (black). e) Mean annual cycle for tracers IVT as obtained from WRF. f) Mean diurnal cycle for IVT as obtained from the WRF simulations (blue) and ERA5 reanalysis (black). g) Mean diurnal cycle for tracers IVT as obtained from WRF.

The noisy tracer IVT signal stands in sharp contrast to the clear diurnal signal of the ET timeseries, highlighting the noisiness of the lower level winds. ET diurnal cycle is stronger than the annual cycle (Fig. 7 a and b). ET peaks during the warm season (November through March). It is important to highlight that the annual cycle in ET is dominated by the signal in the southern Amazon, as the northern Amazon has weak annual variability (?, ?)Fig.4]eiras2020changes. In fact ET in the northern Amazon is sustained during the winter months with greener forests during the dry season (Huete et al., 2006). The diurnal cycle of ET is strong, with high ET values between 18Z and 0Z (14-20 local), associated with enhanced plant photosynthetic activity and higher atmospheric evaporative demand, and negligible nocturnal evapotranspiration. Note that we do not show tracer ET because the tracer flux at the surface is equal to ET, so the signal is the same.

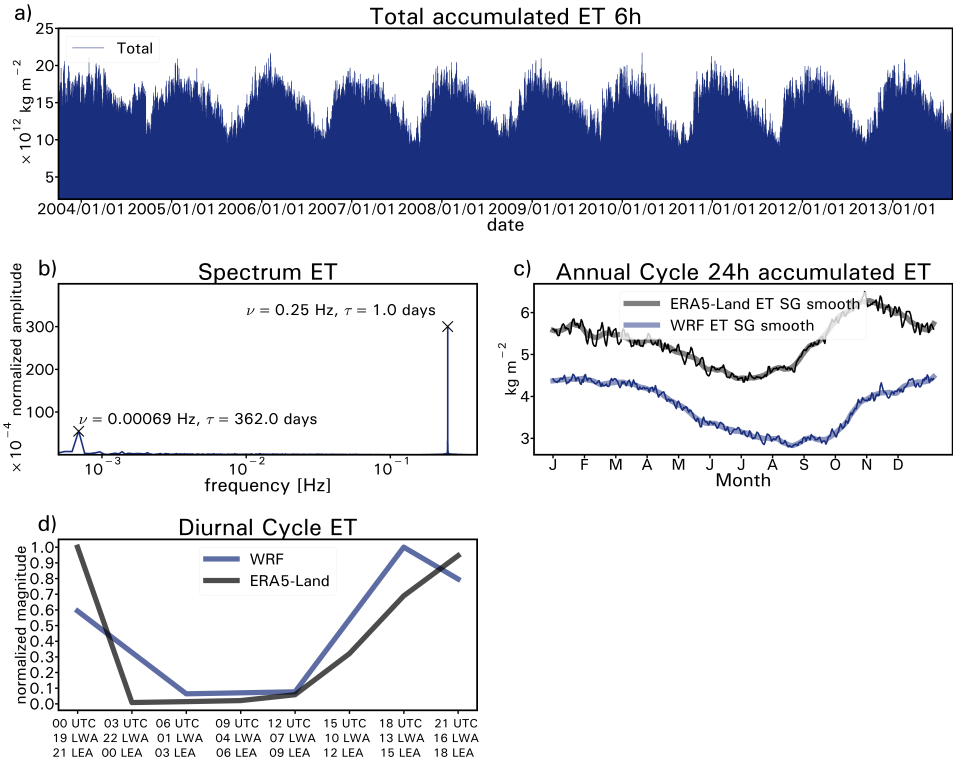

Figure 7. Fast-Fourier transform (FFT) analysis of IVT a) Raw signals of total ET for a 6h-time step time series 2003-2013. b) FFT frequencies spectrum for ET. c) Mean annual cycle for ET as obtained from the WRF simulations (blue) and ERA5-Land reanalysis (black). d) Mean diurnal cycle for IVT as obtained from the WRF simulations (blue) and ERA5-Land reanalysis (black).

4 Discussion and Conclusions

We use the WRF regional climate model with the added capability of water vapor tracers to track the moisture that evapotranspires from the Amazon basin and follow it in space and time until it rains out of the atmospheric column. This method allows us to quantify the amount of precipitable water, precipitation and integrated vapor transport that originates from Amazonian ET, without having to rely on simplifying assumptions of previous estimates. WRF-WVT allows us to analyze local moisture sources at shorter temporal and higher spatial scales than any other existing method. In addition to the annual and semi-annual cycle, our analysis revealed a clear diurnal cycle in all of the moisture budget variables. Our results show that:

- Precipitation of Amazonian origin (or recycled precipitation) has a strong zonal gradient with values gradually increasing towards the western part of the basin, following the prevailing wind patterns. Approximately half of the precipitation near the foothills of the Andes mountains is of Amazonian origin. Interestingly, this region of highest recycling in the Andean foothills is also one of the rainiest regions in the world due to exposure to easterly winds and orographic ascent mechanisms (Espinoza et al., 2015).
- Local evapotranspiration is more efficiently rained out of the column than remote moisture, particularly in the eastern part of the domain. This indicates that the

well mixed assumption used in most analytical recycling models, does not hold throughout the region. It also suggests an effective ascent mechanism in the eastern side of the domain for low-level moisture to contribute to precipitation.

- Climatologically, we find that nearly 30% of Amazonian precipitation comes from Amazonian evapotranspiration. This agrees with previous studies using a wide variety of models. The agreement is rather surprising given the simplifying assumptions in previous estimates, and suggests a robust result: the recycling ratio in the Amazon basin is between 25-35%.
- Recycled precipitation shows a strong annual and 6-month signal. This is related to the ITCZ which passes once a year over the southern Amazon, the region that shows the strongest annual cycle. However, the ITCZ passes twice over the northern Amazon each year, once on its way south around October-November, and once on its way north around April-May (see Eiras-Barca et al. (2020), their Figure 4). ET, on the other hand, only shows a very weak annual cycle. This is related to the ability of the Amazonian forest, particularly in the north, to sustain ET during the dry season (da Rocha et al., 2009). Interestingly, tracer precipitable water shows a clear 6-month signal, unlike total IWV which has both an annual and 6-month signal. This indicates that the high total IWV in December-March is primarily of oceanic origin, not of local origin, this can also be seen with the lower IWV recycling ratios during December-February than in other seasons.
- At the diurnal timescale, water vapor of Amazonian origin increases from early morning into the afternoon as evapotranspired moisture from the plants and soil accumulates in the atmospheric column, then some of this water is rained out through convective precipitation in the early evening. This agrees with observations of IWV and convection in Manaus that reveal that convective events are characterized by an 8 hour period of weak convergence, followed by a 4 hour period of intense convergence followed by a transition from shallow to deep convection (Adams et al., 2013). Later in the night, the water vapor is swept away by nocturnal winds associated with the South American Low Level Jet. When visualized, the diurnal pattern of Amazonian IWV appears as a beating signal `https://www.youtube.com/watch?v=sVP9B_85jfw`.

Our results imply that, compared to the traditional 8-10 day lifetime of water vapor as calculated by global analysis (van der Ent & Tuinenburg, 2017), or even the 4-5 day estimates of (Läderach & Sodemann, 2016) the lifetime of water vapor over the Amazon forest is much shorter. In fact, in global analyses the Amazon basin stands out as having some of the shortest lifetimes and length scales of terrestrial moisture on Earth (van der Ent et al., 2014), with average distance between transpiration and precipitation of about 600km (Staal et al., 2018). So the Amazon has younger atmospheric water than other places in the globe. The efficiency of recycling, short lifetime and length scale of Amazonian moisture also implies that ET of Amazonian origin is less likely to contribute to downwind precipitation than originally thought. In fact, once the air masses leave the Amazonian forest, studies have found an exponential decrease of precipitation with distance (Molina et al., 2019). Future studies should focus on observational validation of these results using observations of water isotopes, with in-situ or remote sensing observations.

Acknowledgments

This research was supported by the National Science Foundation (NSF) CAREER Award AGS 1454089. Visualization by David Bock, Lead Visualization Programmer, National Center for Supercomputing Applications, University of Illinois, Champaign Urbana, IL. Visualizations supported by XSEDE award ATM170030. L.G., R.N. and J.E.B were funded by the Spanish government within the LAGRIMA (RTI2018-095772-B-I00) project, funded by Ministerio de Ciencia, Innovacion y Universidades, Spain, which are also funded by

FEDER (European Regional Development Fund, ERDF). J.E.B was also supported by the Xunta de Galicia (Galician Regional Government) under grant and by the Fulbright Program (US Department of State). Z. Y was supported by the Office of Science of the U.S. Department of Energy (DOE) as part of the Atmospheric System Research (ASR) Program via Grant KP1701000/57131. All results from model simulations are available as: Dominguez, Francina (2021): WRF model output with water vapor tracers over Amazon river basin. University of Illinois at Urbana-Champaign. `https://doi.org/10.13012/B2IDB-8790412_V1`.

References

Adams, D. K., Gutman, S. I., Holub, K. L., & Pereira, D. S. (2013, June). GNSS observations of deep convective time scales in the Amazon. *Geophys. Res. Lett.*, *40*(11), 2818–2823.

Arraut, J. M., Nobre, C., Barbosa, H. M., Obregon, G., & Marengo, J. (2012). Aerial rivers and lakes: looking at large-scale moisture transport and its relation to amazonia and to subtropical rainfall in south america. *Journal of Climate*, *25*(2), 543–556.

Bosilovich, M., & Chern, J. (2006). Simulation of water sources and precipitation recycling for the MacKenzie, Mississippi, and Amazon River basins. *Journal of Hydrometeorology*, *7*(3), 312–329.

Bosilovich, M. G., & Chern, J.-D. (2006). Simulation of water sources and precipitation recycling for the mackenzie, mississippi, and amazon river basins. *Journal of Hydrometeorology*, *7*(3), 312–329.

Brubaker, K. L., Entekhabi, D., & Eagleson, P. (1993). Estimation of continental precipitation recycling. *Journal of Climate*, *6*(6), 1077–1089.

Burde, G. I. (2006). Bulk recycling models with incomplete vertical mixing. part i: Conceptual framework and models. *Journal of climate*, *19*(8), 1461–1472.

da Rocha, H. R., Manzi, A. O., Cabral, O. M., Miller, S. D., Goulden, M. L., Saleska, S. R., ... Maia, J. F. (2009, January). Patterns of water and heat flux across a biome gradient from tropical forest to savanna in Brazil. *J. Geophys. Res.*, *114*, G00B12.

Dee, D. P., Uppala, S. M., Simmons, A., Berrisford, P., Poli, P., Kobayashi, S., ... others (2011). The era-interim reanalysis: Configuration and performance of the data assimilation system. *Quarterly Journal of the royal meteorological society*, *137*(656), 553–597.

Dominguez, F., Hu, H., & Martinez, J. (2020). Two-layer dynamic recycling model (2l-drm): Learning from moisture tracking models of different complexity. *Journal of Hydrometeorology*, *21*(1), 3–16.

Dominguez, F., Kumar, P., Liang, X.-Z., & Ting, M. (2006). Impact of atmospheric moisture storage on precipitation recycling. *Journal of climate*, *19*(8), 1513–1530.

Dominguez, F., Miguez-Macho, G., & Hu, H. (2016). Wrf with water vapor tracers: A study of moisture sources for the north american monsoon. *Journal of Hydrometeorology*, *17*(7), 1915–1927.

Drumond, A., Marengo, J., Ambrizzi, T., Nieto, R., Moreira, L., & Gimeno, L. (2014). The role of the Amazon Basin moisture in the atmospheric branch of the hydrological cycle: a Lagrangian analysis. *Hydrol Earth Syst Sc*, *18*(7), 2577–2598.

Eiras-Barca, J., Dominguez, F., Hu, H., Garaboa-Paz, D., & Miguez-Macho, G. (2017). Evaluation of the moisture sources in two extreme landfalling atmospheric river events using an eulerian wrf tracers tool. *Earth Syst. Dyn*, *8*(4), 1247–1261.

Eiras-Barca, J., Dominguez, F., Yang, Z., Chug, D., Nieto, R., Gimeno, L., & Miguez-Macho, G. (2020). Changes in south american hydroclimate under

projected amazonian deforestation. *Annals of the New York Academy of Sciences*.

Eltahir, E. A., & Bras, R. L. (1994). Precipitation recycling in the amazon basin. *Quarterly Journal of the Royal Meteorological Society*, *120*(518), 861–880.

Espinoza, J. C., Chavez, S., Ronchail, J., Junquas, C., Takahashi, K., & Lavado, W. (2015, May). Rainfall hotspots over the southern tropical Andes: Spatial distribution, rainfall intensity, and relations with large-scale atmospheric circulation. *Water Resour Res*, *51*(5), 3459–3475.

Fan, Y., Miguez-Macho, G., Weaver, C. P., Walko, R., & Robock, A. (2007). Incorporating water table dynamics in climate modeling: 1. water table observations and equilibrium water table simulations. *Journal of Geophysical Research: Atmospheres*, *112*(D10).

Hong, S.-Y., & Lim, J.-O. J. (2006). The wrf single-moment 6-class microphysics scheme (wsm6). *Asia-Pacific Journal of Atmospheric Sciences*, *42*(2), 129–151.

Hong, S.-Y., & Pan, H.-L. (1996). Nonlocal boundary layer vertical diffusion in a medium-range forecast model. *Monthly weather review*, *124*(10), 2322–2339.

Huete, A. R., Didan, K., Shimabukuro, Y. E., Ratana, P., Saleska, S. R., Hutyra, L. R., ... Myneni, R. (2006). Amazon rainforests green-up with sunlight in dry season. *Geophys. Res. Lett.*, *33*(6), L06405–4.

Huffman, G. J., Adler, R. F., Bolvin, D. T., & Nelkin, E. J. (2010). The trmm multi-satellite precipitation analysis (tmpa). In *Satellite rainfall applications for surface hydrology* (pp. 3–22). Springer.

Insua-Costa, D., & Miguez-Macho, G. (2018). A new moisture tagging capability in the weather research and forecasting model: formulation, validation and application to the 2014 great lake-effect snowstorm. *Earth System Dynamics*, *9*(1), 167.

Kain, J. S. (2004). The kain–fritsch convective parameterization: an update. *Journal of applied meteorology*, *43*(1), 170–181.

Kain, J. S., & Fritsch, J. M. (1990). A one-dimensional entraining/detraining plume model and its application in convective parameterization. *Journal of the Atmospheric Sciences*, *47*(23), 2784–2802.

Laderach, A., & Sodemann, H. (2016). A revised picture of the atmospheric moisture residence time. *Geophys. Res. Lett.*, *43*, 924-933.

Läderach, A., & Sodemann, H. (2016, February). A revised picture of the atmospheric moisture residence time. , 1–10.

Lettau, H., Lettau, K., & Molion, L. C. B. (1979). Amazonia's hydrologic cycle and the role of atmospheric recycling in assessing deforestation effects. *Monthly Weather Review*, *107*(3), 227–238.

Martinez, J. A., Dominguez, F., & Miguez-Macho, G. (2016a). Effects of a groundwater scheme on the simulation of soil moisture and evapotranspiration over southern south america. *Journal of Hydrometeorology*, *17*(11), 2941–2957.

Martinez, J. A., Dominguez, F., & Miguez-Macho, G. (2016b). Impacts of a groundwater scheme on hydroclimatological conditions over southern south america. *Journal of Hydrometeorology*, *17*(11), 2959–2978.

Miguez-Macho, G., & Fan, Y. (2012). The role of groundwater in the amazon water cycle: 1. influence on seasonal streamflow, flooding and wetlands. *Journal of Geophysical Research: Atmospheres*, *117*(D15).

Miguez-Macho, G., Fan, Y., Weaver, C. P., Walko, R., & Robock, A. (2007). Incorporating water table dynamics in climate modeling: 2. formulation, validation, and soil moisture simulation. *Journal of Geophysical Research: Atmospheres*, *112*(D13).

Molina, R. D., Salazar, J. F., Martinez, J. A., Villegas, J. C., & Arias, P. A. (2019, March). Forest-Induced Exponential Growth of Precipitation Along Climatological Wind Streamlines Over the Amazon. *J Geophys Res-Atmos*, *124*(5),

2589–2599.

Niu, G.-Y., Yang, Z.-L., Mitchell, K. E., Chen, F., Ek, M. B., Barlage, M., ... others (2011). The community noah land surface model with multiparameterization options (noah-mp): 1. model description and evaluation with local-scale measurements. *Journal of Geophysical Research: Atmospheres*, *116*(D12).

Salati, E., Dall'Olio, A., Matsui, E., & Gat, J. R. (1979). Recycling of water in the amazon basin: an isotopic study. *Water resources research*, *15*(5), 1250–1258.

Salio, P., Nicolini, M., & Saulo, A. (2002). Chaco low-level jet events characterization during the austral summer season. *Journal of Geophysical Research: Atmospheres*, *107*(D24), ACL–32.

Satyamurty, P., da Costa, C. P. W., & Manzi, A. O. (2013). Moisture source for the amazon basin: a study of contrasting years. *Theoretical and Applied Climatology*, *111*(1-2), 195–209.

Segura, H. (2019, June). New insights into the rainfall variability in the tropical Andes on seasonal and interannual time scales. *Clim Dynam*, *53*(1), 405–426.

Staal, A., Tuinenburg, O. A., Bosmans, J. H. C., Holmgren, M., van Nes, E. H., Scheffer, M., ... Dekker, S. C. (2018, May). Forest-rainfall cascades buffer against drought across the Amazon. *Nature Publishing Group*, 1–8.

Tanaka, L. d. S., Satyamurty, P., & Machado, L. A. T. (2014). Diurnal variation of precipitation in central a mazon b asin. *International journal of climatology*, *34*(13), 3574–3584.

Trenberth, K. E. (1999, May). Atmospheric moisture recycling: Role of advection and local evaporation. *J. Climate*, *12*(5), 1368–1381.

Tuinenburg, O., & van der Ent, R. (2019). Land surface processes create patterns in atmospheric residence time of water. *Journal of Geophysical Research: Atmospheres*, *124*(2), 583–600.

van der Ent, R. J., Savenije, H. H. G., Schaefli, B., & Steele-Dunne, S. C. (2010). Origin and fate of atmospheric moisture over continents. *Water Resour Res*, *46*, W09525.

van der Ent, R. J., & Tuinenburg, O. A. (2017). The residence time of water in the atmosphere revisited. *Hydrol. Earth Syst. Sci.*, *21*(2), 779–790.

van der Ent, R. J., Wang-Erlandsson, L., Keys, P. W., & Savenije, H. H. G. (2014). Contrasting roles of interception and transpiration in the hydrological cycle – Part 2: Moisture recycling. *Earth Syst. Dynam.*, *5*(2), 471–489.

Vera, C., Baez, J., Douglas, M., Emmanuel, C., Marengo, J., Meitin, J., ... others (2006). The south american low-level jet experiment. *Bulletin of the American Meteorological Society*, *87*(1), 63–78.

Wilks, D. S. (2011). *Statistical methods in the atmospheric sciences* (Vol. 100). Academic press.

Wu, M., & Lee, J. E. (2019, August). Thresholds for Atmospheric Convection in Amazonian Rainforests. *Geophys. Res. Lett.*, *46*(16), 10024–10033.

Yang, Z., & Dominguez, F. (2019). Investigating land surface effects on the moisture transport over south america with a moisture tagging model. *Journal of Climate*, *32*(19), 6627–6644.

Zemp, D. C., Schleussner, C. F., Barbosa, H. M. J., van der Ent, R. J., Donges, J. F., Heinke, J., ... Rammig, A. (2014). On the importance of cascading moisture recycling in South America. *Atmos. Chem. Phys.*, *14*(23), 13337–13359.